

the drug E-4031, which selectively blocks I_{Kr} (9), inhibits the inward HERG current with an IC_{50} of 588 nM (Fig. 4H), providing a pharmacological link between HERG and I_{Kr} . In contrast, the outward current is relatively resistant to E-4031. The selective sensitivity of the inward current, when the open probability of channels is presumed highest, suggests an open-channel block. The rectification mechanism that limits outward conductance may obstruct E-4031 access to the pore and may explain a recent report of E-4031 insensitivity in expressed HERG channels when an outward current protocol was used (28). These studies suggest that HERG encodes a component of I_{Kr} , but future studies will be necessary to determine the subunit composition and biophysical properties of native channels containing HERG subunits in human cardiac tissue.

REFERENCES AND NOTES

- W. D. Kaplan and W. E. Trout, *Genetics* **61**, 399 (1969); nomenclature for genes and associated polypeptides is according to guidelines in *Trends in Genetics Guide to Genetic Nomenclature* (1995).
- B. Ganetzky and C.-F. Wu, *J. Neurogenet.* **1**, 17 (1983).
- J. W. Warmke, R. Drysdale, B. Ganetzky, *Science* **252**, 1560 (1991).
- G. A. Robertson, J. W. Warmke, B. Ganetzky, *Biophys. J. Abstr.* **64**, A340 (1993).
- A. Bruggemann, L. A. Pardo, W. Stuhmer, O. Pongs, *Nature* **365**, 445 (1993); J. Ludwig et al., *EMBO J.* **13**, 4451 (1994).
- J. W. Warmke and B. Ganetzky, *Proc. Natl. Acad. Sci. U.S.A.* **91**, 3438 (1994).
- This work was previously reported in abstract form M. C. Trudeau, J. W. Warmke, B. Ganetzky, G. A. Robertson, *Biophys. J. Abstr.* **68**, A32 (1995); G. A. Robertson and M. C. Trudeau, *ibid.*, p. A363.
- D. DiFrancesco and D. Noble, *Philos. Trans. R. Soc. London Ser. B* **307**, 353 (1985); G.-N. Tseng, D. Zipes and J. Jalife, Eds., *Cardiac Electrophysiology* (Saunders, Philadelphia, PA, ed. 2, 1995), pp. 260–268.
- M. C. Sanguinetti and N. K. Jurkiewicz, *J. Gen. Physiol.* **96**, 195 (1990).
- Y. Kubo, T. J. Baldwin, Y. N. Jan, L. Y. Jan, *Nature* **362**, 127 (1993); K. Ho et al., *ibid.*, p. 31; F. Perier, C. M. Radeke, C. A. Vandenberg, *Proc. Natl. Acad. Sci. U.S.A.* **91**, 6240 (1994); E. N. Makhina, A. J. Kelly, A. N. Lopatin, R. W. Mercer, C. G. Nichols, *J. Biol. Chem.* **269**, 20468 (1994).
- D. M. Papazian, T. L. Schwarz, B. L. Tempel, Y. N. Jan, L. Y. Jan, *Science* **237**, 749 (1987).
- N. S. Atkinson, G. A. Robertson, B. Ganetzky, *ibid.* **253**, 551 (1991).
- The HERG expression clone was constructed from three incomplete, overlapping gene fragments. One genomic and two cDNA clones (hh10 and hh1) were isolated as described (6). The cDNAs were ligated at a shared Sph I site, resulting in a clone containing all but the first 29 base pairs (bp) of the coding region. The 5' coding region was added by means of three-way polymerase chain reaction (PCR) [O. Landt, H.-P. Grunert, U. Hahn, *Gene* **96**, 125 (1990)]. Primers were directed at the genomic clone to amplify a 76-bp segment containing the 5' end of the coding region and a 47-bp overlap with the 5' end of the hh10-1 fused cDNA. A Barn HI site was also added by means of the 5' primer to facilitate subsequent manipulations. The product of this reaction was used as the 5' primer in the next PCR with the hh10-1-fused cDNA as the template. The 3' primer was complementary to sequence just downstream from a unique Nco I site in the hh10-1-fused cDNA. This reaction provided a 94-bp product containing the 5' coding sequence from the genomic clone linked to the first 622 bp of the fused hh10-1 cDNA. This fragment included flanking Barn HI and Nco I sites, which were used to ligate the fragment to the pGH19 vector and the hh10-1-fused cDNA. The pGH19 expression vector is a modification of the pGEMHE vector [E. R. Liman, J. Tytgat, and J. P. Hess *Neuron* **9**, 861 (1992)].
- Standard protocols for in vitro transcription, injection, and maintenance of oocytes were used [B. Rudy and L. E. Iverson, Eds., *Methods Enzymol.* **207**, 225–390 (1992)].
- S. Hagiwara, S. Miyazaki, N. P. Rosenthal, *J. Gen. Physiol.* **67**, 612 (1976); S. Hagiwara, S. Miyazaki, W. Moody, J. Patlak, *J. Physiol.* **279**, 167 (1978).
- W. Stuhmer et al., *Nature* **339**, 597 (1989); D. Papazian, L. Timpe, Y. N. Jan, L. Y. Jan, *ibid.* **349**, 305 (1991); E. R. Liman, P. Hess, F. Weaver, G. Koren, *ibid.* **353**, 752 (1991).
- T. Hoshi, W. N. Zagotta, R. W. Aldrich, *Science* **250**, 533 (1990).
- C. M. Armstrong and L. Binstock, *J. Gen. Physiol.* **48**, 859 (1965); C. M. Armstrong, *ibid.* **54**, 553 (1969).
- C. Vandenberg, *Proc. Natl. Acad. Sci. U.S.A.* **84**, 2560 (1987); H. Matsuda, A. Saigusa, H. Irisawa, *Nature* **325**, 156 (1987).
- A. N. Lopatin, E. N. Makhina, C. G. Nichols, *Nature* **372**, 366 (1994).
- E. Ficker, M. Tagliafata, B. A. Wible, C. M. Henley, A. M. Brown, *Science* **266**, 1068 (1994).
- T. Hoshi, W. N. Zagotta, R. W. Aldrich, *Neuron* **7**, 547 (1991).
- D. P. Schachtman, J. I. Schroeder, W. J. Lucas, J. A. Anderson, R. F. Gaber, *Science* **258**, 1654 (1992).
- P. C. Zei, A. G. Miller, R. W. Aldrich, *Biophys. J. Abstr.* **68**, A32 (1995).
- M. E. Curran et al., *Cell* **80**, 795 (1995).
- P. F. Cranefield and R. S. Aronson, in P. F. Cranefield, R. S. Aronson, Eds., *Cardiac Arrhythmias: The Role of Triggered Activity and Other Arrhythmias* (Future, Mount Kisco, NY, 1988), pp. 553–579.
- L. V. Buchanan, G. Kabell, M. N. Brunden, J. K. Gibson, *J. Cardiovasc. Pharmacol.* **22**, 540 (1993).
- M. C. Sanguinetti, C. Jiang, M. E. Curran, M. T. Keating, *Cell* **81**, 299 (1995).
- Linear leak was determined by stepping from -80 mV to -100 mV and -120 mV in solutions containing 10 mM or greater $[K]_o$. Under these conditions no conductance due to active currents could be measured (by direct observation or tail current analysis). Most records used for this study had leaks under these conditions of $<2\%$ peak currents and were therefore not leak subtracted.
- We thank R. Fettiplace, M. Jackson, C. January, P. Lipton, P. Smith, and J. Wang for comments on the manuscript, E. Goulding and S. Siegelbaum for the pGH19 expression vector, and C. January for E-4031 and many helpful discussions. Supported by the American Heart Association of Wisconsin and the Wisconsin Alumni Research Foundation (G.A.R.) and by the NIH (B.G.) and the Muscular Dystrophy Association (J.W.W.).

27 March 1995; accepted 26 May 1995

Spatial Memory of Body Linear Displacement: What Is Being Stored?

Alain Berthoz, Isabelle Israël*, Pierre Georges-François, Renato Grasso, Toshihiro Tsuzuku

The ability to evaluate traveled distance is common to most animal species. Head trajectory in space is measured on the basis of the converging signals of the visual, vestibular, and somatosensory systems, together with efferent copies of motor commands. Recent evidence from human studies has shown that head trajectory in space can be stored in spatial memory. A fundamental question, however, remains unanswered: How is movement stored? In this study, humans who were asked to reproduce passive linear whole-body displacement distances while blindfolded were also able to reproduce velocity profiles. This finding suggests that a spatiotemporal dynamic pattern of motion is stored and can be retrieved with the use of vestibular and somesthetic cues.

Active or passive whole-body displacement is estimated by convergent signals from the vestibular system, vision, proprioception, and efferent copies of motor commands (1, 2). The reconstruction of the experienced trajectory, called path integration (3), allows a return to the departure point, that is, homing (3–5). The term "integration" could correspond to the hypothesis that the brain computes distance either by cumulating successive positions along the path (3) or through temporal integration of velocity or acceleration. An alternate hypothesis is that the brain stores a

Laboratoire de Physiologie de la Perception et de l'Action, Collège de France—Centre National de la Recherche Scientifique (CNRS), 11 Place Mercelin Berthollet, 75006 Paris, France.

*To whom correspondence should be addressed.

spatiotemporal profile of motion and replays it during return.

Different species perform path integration in different ways. In humans, linear and angular passive whole-body displacements can be stored in spatial memory (6, 7) and retrieved to generate accurate saccades to remembered targets (8–11); some cortical areas involved in this self-motion memory have been identified (12). Although the contribution of otoliths in small mammals has been debated (4, 13), healthy humans can correctly estimate a linear distance after passive transport (7, 9, 14); this performance is degraded in the absence of the vestibular system, at least for small distances (9).

One main question, however, remains unanswered: How is movement stored? Is it

in the form of information relating to the distance traveled (for example, a vector), or is it a dynamic record of changes in velocity over time? To date, there has been no clear demonstration of the capacity of humans to perform path integration during linear motion. Here, we used a mobile robot (Fig. 1A) (15) and devised a paradigm that enabled us to approach this question in a way that previous tasks (7, 9) could not.

Twelve healthy volunteers (20 to 50 years old) participated in the first experiment in accord with the ethical committee of the CNRS. The participants were seated on the robot (Fig. 1A) and were trained to use a joystick to control its velocity; they were left free to move forward along a 50-m corridor until they felt confident in manipulating the robot in the light, with their heads restrained and with headphones on (15). Each participant was then passively transported forward along the naso-occipital axis while blindfolded. A displacement of 2, 4, 6, 8, or 10 m was imposed in random sequence. After the robot came to a complete stop, the experimenter touched the participant's shoulder. This was the signal for the participant to drive the robot with the joystick in the same direction (forward) and to attempt to reproduce, as accurately as possible, the distance previously imposed.

In the first experiment, the stimulus acceleration was square-shaped (range 0.06 to 1 m/s²), with a subsequent deceleration of identical form and magnitude. The resulting velocity profiles were triangular, with a peak velocity range of 0.6 to 1 m/s (Fig. 1B). Although the response distances revealed some interindividual variability (Fig. 2A), most of the participants (10 of 12) reproduced velocity profiles that were approximately triangular in shape (Fig. 2B).

Only one participant overshot the maximal velocity of the stimulus; his response was a

step velocity profile of short duration that led to an accurate reproduced distance (final position 19.06 m, instead of the expected 20 m) (Fig. 2).

The average regression line and the means and SDs of the reproduced distances are shown in Fig. 3, along with the 12 participants' individual regression lines. The equation for the average stimulus (S)-response (R) regression line was $R = 0.86S + 0.47$ m. The correlation coefficient was highly significant ($P < 0.0005$) for all participants, and linear regression was a good predictor of the true relation ($r^2 = 0.87 \pm 0.08$, mean \pm SD; SE of the estimate = 1.01 \pm 0.38 m). A 35-year-old male with paraplegia (from a spinal cord section 10 years earlier) also participated in the test, and his performance was similar to that of the healthy participants ($R = 0.74S + 0.40$ m; $r^2 = 0.81$); although this participant could still perceive tactile cues through his trunk, this result suggested that the detection of robot vibrations by the lower part of the body did not represent an important cue in this task.

The duration of the triangular velocity profiles could have provided information that helped participants to reproduce distances accurately. Indeed, there was a fairly good linear regression ($R = 0.80S + 1.34$ s) between stimulus and response duration ($r^2 = 0.80 \pm 0.09$). To eliminate the possible role of duration evaluation in distance reproduction, we designed a second experiment in which the stimulus duration was kept constant (16 s) over the different distances. The participants, seven members of the volunteer group from the first experiment 4 months earlier, received no retraining in the use of the robot. Different peak velocities and trapezoidal or squarelike velocity profiles were used (Fig. 1C). In addition, to test the reproducibility of responses between the two experiments, we administered five trials with

triangular velocity profiles; the stimulus-response linear regression was $R = 0.96S + 0.51$ m ($r^2 = 0.92 \pm 0.05$; SE of the estimate = 0.95 \pm 0.41 m), which indicated no difference with the first experiment.

With the constant duration stimuli, participants were able to reproduce the imposed distance as in the first experiment, whatever the velocity profile. The average linear regression line was $R = 0.89S + 0.84$ m ($r^2 = 0.86 \pm 0.12$) with the squarelike profile, and $R = 0.90S + 0.75$ m ($r^2 = 0.88 \pm 0.09$) with the trapezoidal profile. Therefore, the

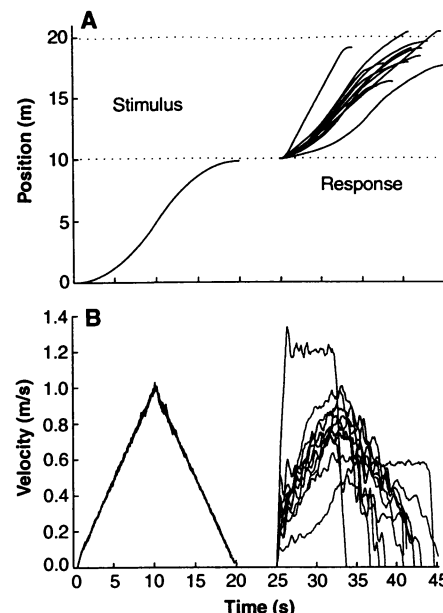


Fig. 2. (A) Illustration of the paradigm, with the odometry recorded from the same trial performed by the 12 participants. (B) Linear velocities computed from the position traces of (A).

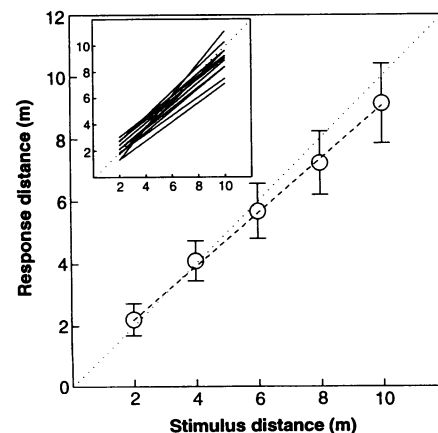
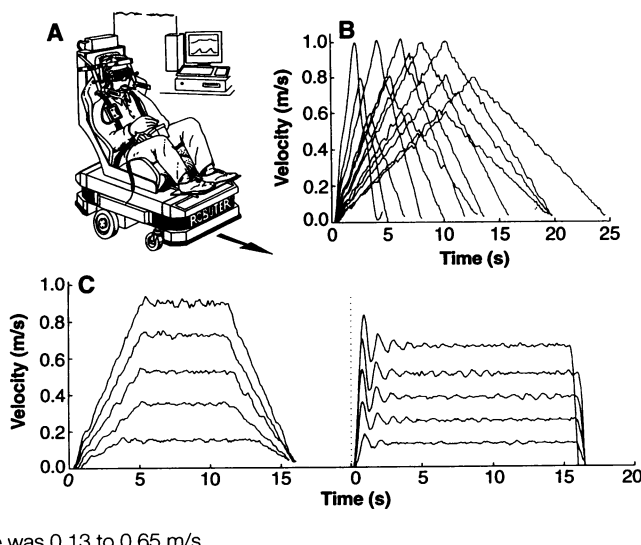


Fig. 3. Participants' performance in the first experiment (triangular velocity profile). The dashed line represents the mean of the 12 individual regression lines (inset), and the regression coefficient ($r^2 = 0.87$) is the mean value for all participants. Superimposed are the means and SDs of the 12 participants' mean responses to each stimulus. The dotted line is the diagonal.

duration information provided in the first experiment was not necessary for the participants to correctly reproduce the imposed distance. The response duration for both velocity patterns was 14.5 ± 3.15 s ($n = 14$). The participant who exhibited short step responses in the first experiment (Fig. 2) did the same in the constant duration experiment, with a mean response duration of 7.6 s for both stimulus velocity patterns.

In the second experiment (Fig. 4), the participants tended to reproduce the waveform of the imposed velocity profile, as they did with the triangular profile in the first experiment. They reproduced the square and triangular velocity profiles even though they were instructed simply to reproduce distance, not velocity or duration. Although the response to the trapezoidal stimulus was not an accurate copy of the imposed profile, it resembled a trapezoid more than it resembled the other two waveforms.

To test whether reproduction of the velocity profile was necessary for reproduction

of the imposed distance, we asked two participants to perform the task over the same distances (2 to 10 m) with complex velocity profiles that were a random sequence of triangular, square, and trapezoidal patterns. Participants were unable to reproduce these velocity profiles, despite tactile cues. A possible explanation is that although the robot was always moving forward, the participants may have partially misperceived the direction of motion because of the ambiguous nature of otolith signals, which cannot differentiate between acceleration in one direction and deceleration in the other. The stimulus-response individual regression lines were well out of the range of the previous experiments, which suggests that the reproduction of the velocity profile was indeed crucial in the designed task.

These results demonstrate that healthy humans can actively reproduce a passive linear transport of a simple dynamic profile without visual or auditory cues, using only vestibular and somatosensory cues, and that they can reproduce the transported distances remarkably accurately, with small interindividual variability. The reason why the slope of the regression lines was less than 1 can probably be attributed to the so-called range effect, which is often observed in psychophysics experiments (16). The strategy for reproducing the imposed distance most commonly used by the participants was reproduction of the stimulus velocity profile (which implies reproduction of distance, duration, and acceleration). Indeed, data from motion perception and eye movement studies in humans (17) indicate that integration over time of the otolith-induced neural discharge, leading to a close relation between perceived and actual linear velocity (18), occurs over the whole frequency range of the stimuli used in this study. If this is the case, in our experiments the most straightforward way for the participant to reproduce the imposed distance would be to match directly the velocity perceived during reproduction with the velocity profile memorized during passive transport.

Tactile cues may complement the vestibular information by providing signals related to the rate of change of body speed (for example, pressure on the back) as well as signals generated by robot vibrations. All these signals may have been correlated with visually perceived velocity during the training period, allowing a sort of calibration. However, the training procedure probably did not influence the strategy of reproduction, because the performance of the participants in the second experiment was not affected even though no training took place.

The hypothesis that a trajectory can be

recovered from successive positions ignores the role of time, whereas in our first experiment, participants reproduced durations as well as distances. The hypothesis that a static estimate of distance is provided by simple time integration of velocity or acceleration does not take into account the time-dependent evolution of motion; in our experiments, most participants reproduced the overall velocity profiles, which is of course impossible with a static estimate of distance. We therefore believe that our results strongly favor the hypothesis that the brain stores the dynamic properties of whole-body passive linear motion. Although the neuronal mechanisms of path integration have yet to be explored, this interpretation is supported by studies of monkey hippocampal neuronal activity, which was found to correlate with passive linear motion in darkness (19), and of rat hippocampal neuronal discharge, which was shown to be influenced by active motion dynamics (speed, direction, and turning angle) (20). These findings clearly suggest that vestibular and somatosensory incoming signals allow a real-time updating of the internal representation of the position and direction of the body in space.

REFERENCES AND NOTES

- D. I. McCloskey, in *Handbook of Physiology: The Nervous System, vol. II, Motor Control*, V. B. Brooks, Ed. (American Physiological Society, Bethesda, MD, 1981), part 2, pp. 1391–1415.
- S. Glasauer, M. A. Amorim, E. Vitte, A. Berthoz, *Exp. Brain Res.* **98**, 323 (1994).
- M. L. Mittelstaedt and H. Mittelstaedt, *Naturwissenschaften* **67**, 566 (1980).
- H. Mittelstaedt and M. L. Mittelstaedt, in *Avian Navigation*, F. Papi and H. G. Wallraff, Eds. (Springer-Verlag, Berlin and Heidelberg, 1982), pp. 290–297.
- A. S. Etienne, R. Maurer, F. Saucy, E. Teroni, *Anim. Behav.* **34**, 696 (1986); G. V. T. Matthews, *J. Exp. Biol.* **28**, 508 (1951); T. Guilford, *Nature* **363**, 112 (1993).
- F. E. Guedry and C. S. Harris, "Labyrinthine function related to experiments on the parallel swing" (joint report of the U.S. Naval School of Aviation Medicine and National Aeronautics and Space Administration, Bureau of Medicine and Surgery Project MR005.13-6001, 1963); J. S. Beritoff, in *Neural Mechanisms of Higher Vertebrate Behavior*, W. T. Liberson, Ed. (Little, Brown, Boston, 1965), pp. 107–123; S. Miller, M. Potegal, L. Abraham, *Physiol. Psychol.* **11**, 1 (1983); M. Potegal, in *Spatial Abilities: Development and Physiological Foundations*, M. Potegal, Ed. (Academic Press, New York, 1982), pp. 361–387; T. Metcalfe and M. A. Gresty, *Ann. N.Y. Acad. Sci.* **656**, 695 (1992); I. Israël, D. Sievering, E. Koenig, *Acta Otolaryngol.* **115**, 3 (1995).
- I. Israël, N. Chapuis, S. Glasauer, O. Charade, A. Berthoz, *J. Neurophysiol.* **70**, 1270 (1993).
- J. Bloomberg, G. Melville Jones, B. N. Segal, S. McFarlane, J. Soul, *Adv. Oto-Rhino-Laryngol.* **40**, 71 (1988); J. Bloomberg, G. Melville Jones, B. N. Segal, *Exp. Brain Res.* **84**, 47 (1991); A. Berthoz, I. Israël, T. Vieville, D. S. Zee, *Neurosci. Lett.* **82**, 285 (1987); A. Berthoz, I. Israël, D. S. Zee, E. Vitte, *Adv. Oto-Rhino-Laryngol.* **41**, 76 (1988).
- I. Israël and A. Berthoz, *J. Neurophysiol.* **62**, 247 (1989).
- I. Israël, S. Pivaud, C. Pierrot-Deseilligny, A. Berthoz, in *Tutorials in Motor Neuroscience*, J. Requin and G. E. Stelmach, Eds. (Kluwer Academic, Norwell, MA, 1991), pp. 599–607; I. Israël and A. Berthoz, in *Tu-*

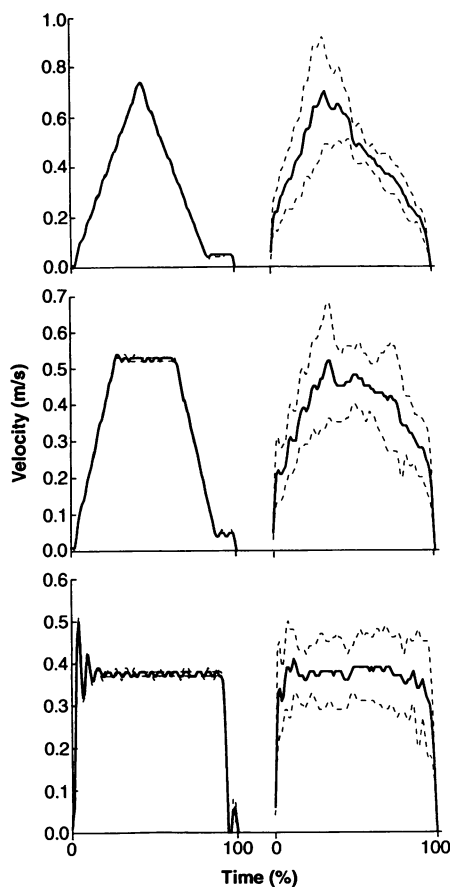


Fig. 4. Mean (solid line) \pm SD (dashed lines) of the stimuli (left) and responses (right) for the three velocity profiles in the second experiment (stimulus distance, 6 m). The time scales for the imposed and reproduced segments were normalized separately. This normalization did not superimpose the peak velocity of all trials at the same point in time.

- torials in Motor Behavior II*, G. E. Stelmach and J. Requin, Eds. (Elsevier North-Holland, Amsterdam, 1992), pp. 195–209.
11. I. Israël, M. Fetter, E. Koenig, *Exp. Brain Res.* **96**, 335 (1993).
 12. I. Israël, S. Rivaud, A. Berthoz, C. Pierrot-Deseilligny, *Ann. N.Y. Acad. Sci.* **656**, 472 (1992); C. Pierrot-Deseilligny, I. Israël, A. Berthoz, S. Rivaud, B. Gaymard, *Exp. Brain Res.* **95**, 166 (1993); I. Israël, A. Berthoz, S. Rivaud, C. Pierrot-Deseilligny, *Brain*, in press.
 13. A. S. Etienne, R. Maurer, F. Saucy, *Behaviour* **106**, 81 (1988).
 14. M. L. Mittelstaedt and S. Glasauer, *Zool. Jahrb. Physiol.* **95**, 427 (1991).
 15. The two front wheels of the robot are driven by two independent 300-W motors that ensure propulsion of a 120-kg maximal mass at a maximal linear velocity of 1.2 m/s, with a maximal acceleration of 1 m/s². Steering is achieved by controlling the relative speed of the two drive wheels. The robot can be controlled either remotely (by a personal computer through a wireless modem) or directly (by a joystick on the robot itself). The joystick controls the robot's linear velocity at steps of 0.05 m/s (robot velocity directly proportional to joystick angle), with a 0.2-s delay. Positioning accuracy and linearity of the trajectory are ensured by proportional integral derivative control loops operating at 100 Hz (using optical encoding of position with a resolution of 1 mm) and a trajectory generation and control algorithm operating at 250 Hz. Participants were secured to the seat by means of three safety belts. Their heads were restrained by a cushioned support (to impede displacements and yaw rotations) and a bite bar (to prevent pitch rotations). They also wore headphones that relayed a wide-band noise ('pink' noise) to prevent perception of external acoustic cues, as well as a pair of goggles with blacked-out lenses to suppress visual information. Optically encoded digital odometry (50 Hz) was transferred from the robot through the modem to the computer after each trial.
 16. E. C. Poulton, in *Handbook of Physiology: The Nervous System*, vol. II, *Motor Control*, V. B. Brooks, Ed. (American Physiological Society, Bethesda, MD, 1981), part 2, pp. 1337–1389; S. S. Stevens, *Am. Sci.* **48**, 226 (1960).
 17. L. R. Young and J. L. Meiry, *Aviat. Space Environ. Med.* **39**, 606 (1968); B. K. Lichtenberg, L. R. Young, A. P. Arrott, *Exp. Brain Res.* **48**, 127 (1982); M. Shelhamer and L. R. Young, *J. Vestib. Res.* **4**, 1 (1994).
 18. L. R. Young, in *Handbook of Physiology: The Nervous System*, vol. III, *Sensory Processes*, I. Darian-Smith, Ed. (American Physiological Society, Bethesda, MD, 1984), part 2, pp. 978–1023.
 19. S. M. O'Mara, E. T. Rolls, A. Berthoz, R. P. Kesner, *J. Neurosci.* **14**, 6511 (1994).
 20. B. L. McNaughton, C. A. Barnes, J. O'Keefe, *Exp. Brain Res.* **52**, 41 (1983); S. I. Wiener, C. A. Paul, H. Eichenbaum, *J. Neurosci.* **9**, 2737 (1989); B. L. McNaughton, L. L. Chen, E. J. Markus, *J. Cogn. Neurosci.* **3**, 190 (1991); S. I. Wiener and A. Berthoz, in *Multisensory Control of Movement*, A. Berthoz, Ed. (Oxford Univ. Press, Oxford, 1993), pp. 427–455; P. E. Sharp, H. T. Blair, D. Etkin, D. B. Tzanatos, *J. Neurosci.* **15**, 173 (1995).
 21. We thank S. Glasauer for computer software design, A. Treffel for adapting the Robuter, and the Association des Paralysés de France and the Cercle Sportif des Invalides (Paris, France) for their kind cooperation. Supported by the European Economic Community (EEC) Esprit Basic Research program, project 6615 (Multisensory Control of Movement); the Cogniscience program (Axe Thématique: Représentation de l'Espace, CNRS, France); an EEC Human Capital and Mobility grant (R.G.); and a grant from the Fyssen Foundation (T.T.).

4 January 1995; accepted 17 April 1995

retinal axons entering the ventral hypothalamus encounter a population of early generated neurons arranged as an inverted V-shaped array pointing anteriorly at the future site of the chiasm (3). These are among the first neurons generated in the embryonic mouse brain (4) and are already present in the ventral hypothalamus at embryonic day 11 (E11), 1.5 days before the arrival of the first retinal axons (3). Axons leaving the optic nerves make a medio-posterior turn toward these embryonic chiasm neurons and their processes. Upon reaching these neurons, retinal axons intermix with and run within the most anterior elements of this array to cross the midline to the other side. In this manner, retinal axons from the two eyes cross over each other to form the X-shaped optic chiasm.

Chiasm neurons express cell surface molecules capable of influencing retinal axon growth. These include L1, a member of the immunoglobulin (Ig) superfamily, which has been shown to be a potent promoter of retinal axon outgrowth in vitro (5) and CD44, a transmembrane glycoprotein known to bind components of the extracellular matrix (6), which exerts a negative influence on embryonic retinal axon outgrowth in vitro (3). These findings suggest that these early-generated neurons may play a role in the initial formation of the X-shaped optic chiasm.

To determine whether these neurons are involved in the establishment of the optic chiasm in vivo, we used a monoclonal antibody (mAb) to CD44 to direct complement-mediated ablation of these cells in E11 mouse embryos in utero before the arrival of retinal axons at the ventral hypothalamus. Embryos were then allowed to develop in utero until E16, an age when retinal axons have formed a well-defined X-shaped optic chiasm in normal animals.

For neuronal ablation, a rat mAb that recognizes mouse CD44 (7) was injected with guinea pig complement into the lateral and third ventricles of E11 mouse embryos ($n = 22$) (8). Antibodies labeled the CD44⁺ chiasm neurons within 4 hours (Fig. 1, B and D) (9). As described previously (3), labeled neurons were organized in a layerlike fashion below the pial surface of the ventral hypothalamus (arrowheads, Fig. 1D), forming a subset of the cells present (Fig. 1E). Twenty-four hours after ablation, very few CD44⁺ chiasm neurons could be visualized with antibody to CD44 (Fig. 1F), although the overall cell density in this region was not detectably reduced (Fig. 1G). Dil(1,1'-diocadecyl-3,3',3'-tetramethylindocarbocyanine perchlorate deposited at the ventral hypothalamic midline in normal embryos labels the axons of the CD44⁺ chiasm

Disruption of Retinal Axon Ingrowth by Ablation of Embryonic Mouse Optic Chiasm Neurons

D. W. Sretavan*, E. Puré, M. W. Siegel, L. F. Reichardt

Mouse retinal ganglion cell axons growing from the eye encounter embryonic neurons at the future site of the optic chiasm. After in vivo ablation of these chiasm neurons with a monoclonal antibody and complement, retinal axons did not cross the midline and stalled at approximately the entry site into the chiasm region. Thus, in the mouse, the presence of early-generated neurons that reside at the site of the future chiasm is required for formation of the optic chiasm by retinal ganglion cell axons.

During embryonic mammalian development, retinal ganglion cell axons exit the optic nerves to grow into the site of the future ventral hypothalamus (1). There, axons from the two eyes, upon leaving the optic nerves, turn within the neuroepithelial

lum in a medio-posterior direction to meet each other and lay down an X-shaped pattern of intersecting retinal axon pathways known as the optic chiasm. Subsequently, retinal axons arriving later undertake a second task in which axons originating from the nasal retina project across the midline to the opposite side of the brain, whereas a group of axons from the temporal retina turn away from the chiasm midline to project toward ipsilateral targets. Ipsilateral and contralateral axon routing appear to involve interactions of retinal growth cones with guidance cues present in the neuroepithelial environment of the optic chiasm (2).

Previous work has shown that the first

D. W. Sretavan, Neuroscience Program, Department of Ophthalmology, and Department of Physiology, University of California, San Francisco, CA 94143, USA.

E. Puré, Wistar Institute, Philadelphia, PA 19104, USA. M. W. Siegel, Department of Pharmacokinetics and Metabolism, Genentech, South San Francisco, CA 94080, USA.

L. F. Reichardt, Neuroscience Program, Department of Physiology, and Howard Hughes Medical Institute, University of California, San Francisco, CA 94143, USA.

*To whom correspondence should be addressed at Department of Ophthalmology K107, University of California, 10 Kirkham Street, San Francisco, CA 94143, USA.